

Manuscript submitted to Environmental Science: Nano

SUPPORTING INFORMATION

Adsorption of selenium(VI) onto transition alumina

Norbert Jordan^{1,*}, Carola Franzen¹, Johannes Lützenkirchen², Harald Foerstendorf¹,
David Hering³, Stephan Weiss¹, Karsten Heim¹, Vinzenz Brendler¹

¹Helmholtz-Zentrum Dresden - Rossendorf (HZDR), Institute of Resource Ecology, Bautzner
Landstraße 400, 01328 Dresden (Germany)

²Institute for Nuclear Waste Disposal, Karlsruhe Institute of Technology (KIT), Hermann-von-
Helmholtz Platz 1, 76344 Eggenstein-Leopoldshafen (Germany)

³current affiliation: sunfire GmbH
Gasanstaltstraße 2, 01237 Dresden, Germany

*Corresponding author:

Phone: +49 351 260 2148, e-mail: n.jordan@hzdr.de

This supporting information contains 19 pages, 10 figures and 1 table.

XRD of raw transition alumina

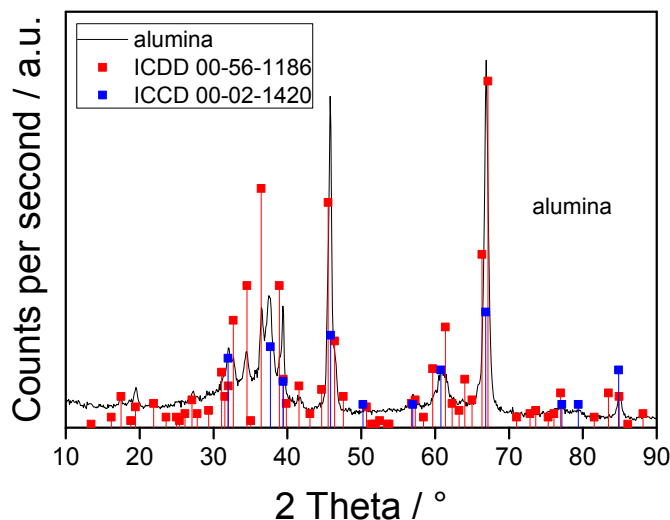


Figure S1. X-ray diffraction pattern of nano transition alumina at room temperature compared with the ICDD cards 00-056-1186 and 00-02-1420.

The Al_2O_3 sample was characterized by XRD on a D8 Bruker-AXS diffractometer equipped with a graphite secondary monochromator, using $\text{Cu K}\alpha$ radiation ($\lambda = 1.5406 \text{ \AA}$) and operating in diffraction mode at 40 kV and 40 mA. Samples were step-scanned in the 2θ range of $20\text{--}90^\circ$ in steps of 0.05° (15 s per step). By comparing the XRD patterns to the International Centre for Diffraction Data (ICDD) cards (Figure S1), the sample was identified as a polycrystalline phase mixture of $\gamma\text{-Al}_2\text{O}_3$ (ICDD 00-002-1420) and $\delta\text{-Al}_2\text{O}_3$ (00-056-1186) in a ratio of approximately 30:70.

Effect of aging on the surface properties of transition–Al₂O₃

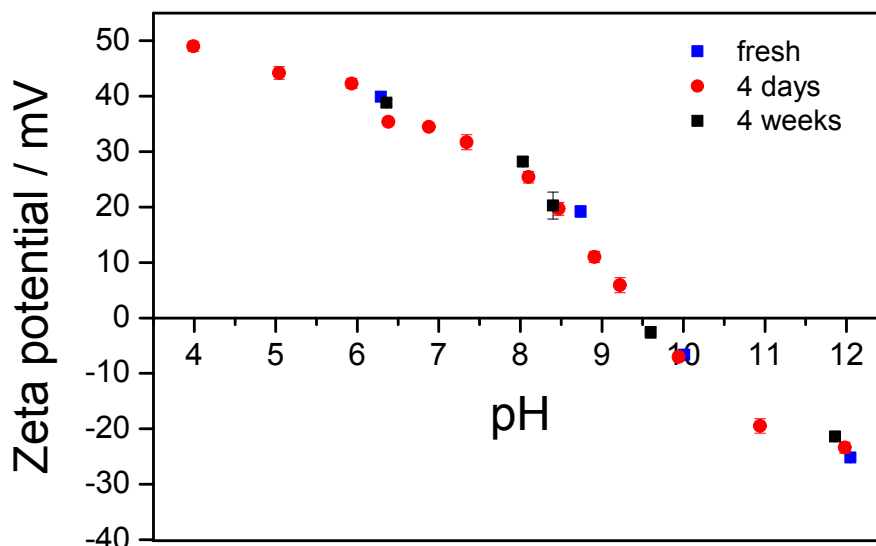


Figure S2. Zeta potential of transition alumina as a function of pH and time at 25 °C (m/v = 0.2 g·L⁻¹, 0.1 mol·L⁻¹ NaCl).

Alumina was suspended in 50 mL polypropylene tubes in the presence of 40 mL of 0.1 mol·L⁻¹ NaCl solution (Merck, p.a.), yielding a mass to volume ratio m/v of 0.2 g·L⁻¹. Samples were prepared in ambient air, since no impact of atmospherically derived carbonate on the zeta potential was observed in preliminary investigations. Suspensions were stirred and the pH values of the oxide suspensions were adjusted using either 0.1 or 0.01 mol·L⁻¹ HCl or NaOH. Each sample was ultrasonicated for 15 s with an ultrasonic finger (Sonopulse HD 2200, Bandelin) prior to measurement. An aliquot of approximately 1 mL was then transferred into a rectangular capillary cell made of polycarbonate with gold plated copper beryllium electrodes. A voltage of 50 V was applied across them. After 2 min of equilibration, the electrophoretic mobility of the suspension was measured at 25 °C. The measured velocity of the particle in the electric field was converted to zeta potential using the Smoluchowski equation. The zeta potential was calculated

Manuscript submitted to Environmental Science: Nano

by the Zetasizer 6.01 software. The reported values were averaged over at least ten measurements.

Potentiometric titrations

Potentiometric titrations (pH range 5 to 9.5) were performed at 25 °C at different ionic strengths of NaCl (0.1, 0.05 and 0.01 mol L⁻¹) with a Metrohm 736 GP Titrino titrator. For each titration, a 30 g L⁻¹ suspension of nano transition alumina (50 mL volume) was inserted into a borosilicate vessel and equilibrated over night at pH ~5. A continuous argon flux (Argon N50 from Air Liquide) was applied over the suspension to minimize intrusion of atmospheric CO₂. To ensure a homogeneous suspension, a Teflon propeller was used. After overnight pre-equilibration, titration by base was performed by addition of aliquots (20 μL) of 0.1 mol L⁻¹ NaOH. The pH electrode (Schott BlueLine 11pH) was calibrated using a three-point calibration with buffer solutions (pH 4.01, 6.87 and 9.18).

FT-IR studies

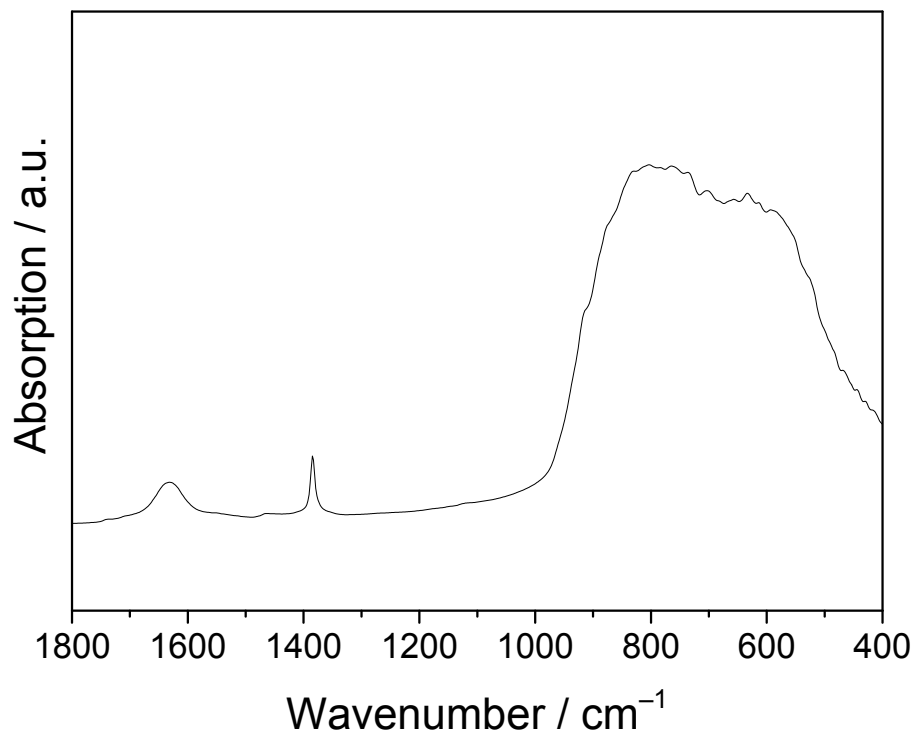


Figure S3. IR spectrum of transition alumina measured in a KBr matrix.

IR spectra of Se(VI) sorption and desorption processes and dependence on ionic strength

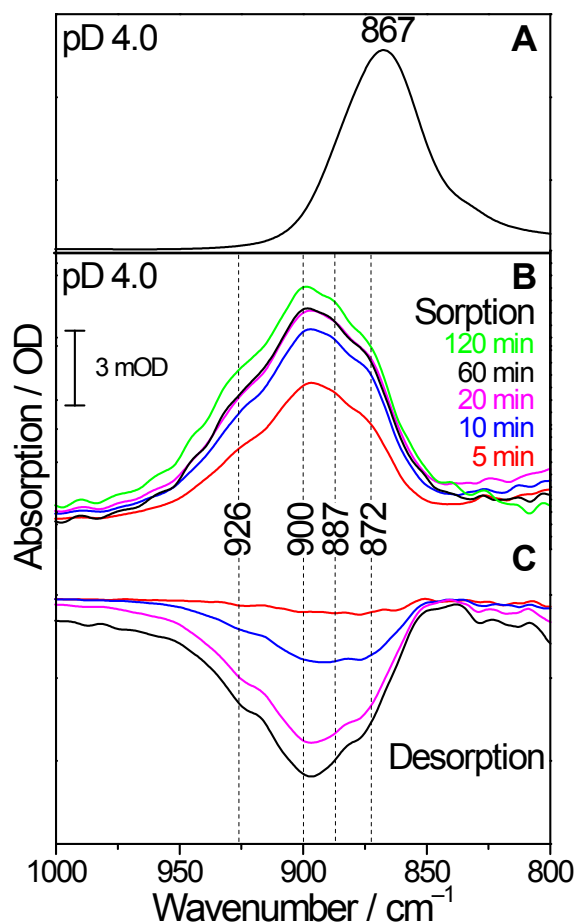


Figure S4. (a) IR spectrum of $0.1 \text{ mol}\cdot\text{L}^{-1}$ selenium(VI) in aqueous solution at $0.1 \text{ mol}\cdot\text{L}^{-1}$ NaCl in D_2O . (b) *In situ* IR spectra taken during selenium(VI) adsorption onto transition alumina ($[\text{Se(VI)}]_{\text{initial}} = 5 \times 10^{-4} \text{ mol}\cdot\text{L}^{-1}$, D_2O , pD 4.0, $0.1 \text{ mol}\cdot\text{L}^{-1}$ NaCl, N_2) at different times. (c) *In situ* IR spectra during release of selenium(VI) at different times after starting to flush the transition alumina phase with blank solution (D_2O , pD 4.0, $0.1 \text{ mol}\cdot\text{L}^{-1}$ NaCl, N_2).

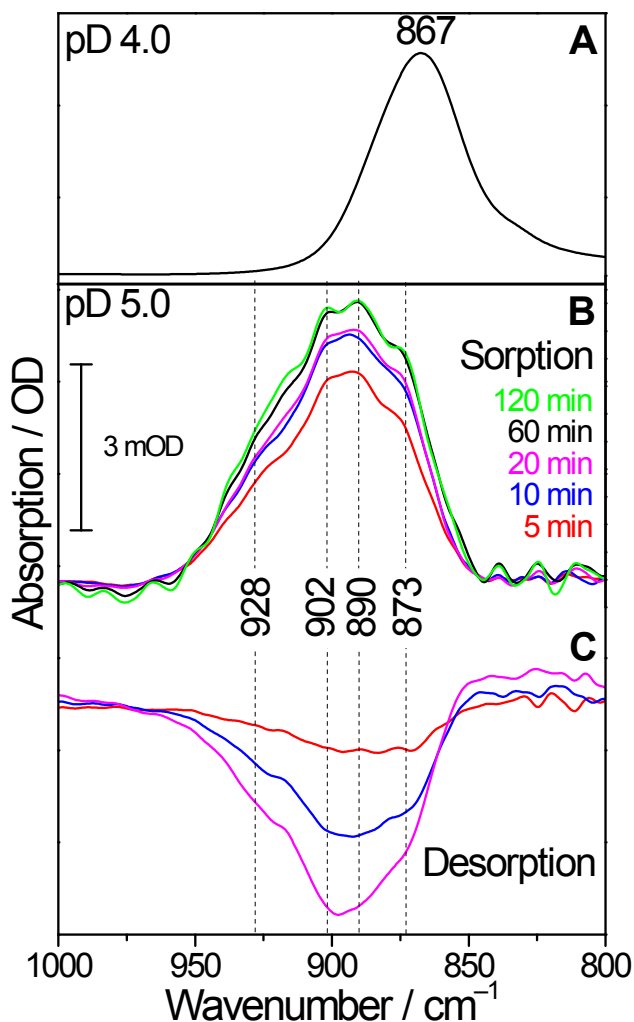


Figure S5. (a) IR spectrum of $0.1 \text{ mol}\cdot\text{L}^{-1}$ selenium(VI) in aqueous solution at $0.1 \text{ mol}\cdot\text{L}^{-1}$ NaCl in D_2O . (b) *In situ* IR spectra taken during selenium(VI) adsorption onto transition alumina ($[\text{Se(VI)}]_{\text{initial}} = 5 \times 10^{-4} \text{ mol L}^{-1}$, D_2O , pD 5.0, $0.1 \text{ mol}\cdot\text{L}^{-1}$ NaCl, N_2) at different times. (c) *In situ* IR spectra during release of selenium(VI) at different times after starting to flush the transition alumina phase with blank solution (D_2O , pD 5.0, $0.1 \text{ mol}\cdot\text{L}^{-1}$ NaCl, N_2).

The increase of the amplitudes 60 minutes after initiating the adsorption (Figure S5B) is only apparent because a continuous background drift occurred throughout the *in situ* experiment. This drift has an almost linear contribution to the amplitudes of the spectra with time, thus, becoming

obvious with increasing acquisition time. In fact, already after 20 min the spectra did not show a significant increase of the amplitudes as can be derived from Figures S5C.

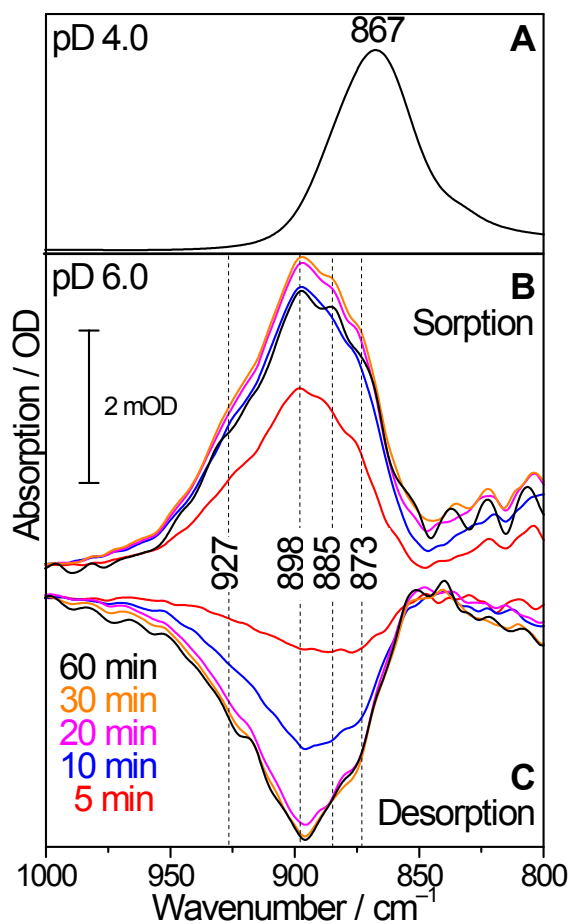


Figure S6. (a) IR spectrum of 0.1 mol·L⁻¹ selenium(VI) in aqueous solution at 0.1 mol·L⁻¹ NaCl in D₂O. (b) *In situ* IR spectra taken during selenium(VI) adsorption onto transition alumina ([Se(VI)]_{initial} = 5 × 10⁻⁴ mol·L⁻¹, D₂O, pD 6.0, 0.1 mol·L⁻¹ NaCl, N₂) at different times. (c) *In situ* IR spectra during release of selenium(VI) at different times after starting to flush the transition alumina phase with blank solution (D₂O, pD 6.0, 0.1 mol·L⁻¹ NaCl, N₂).

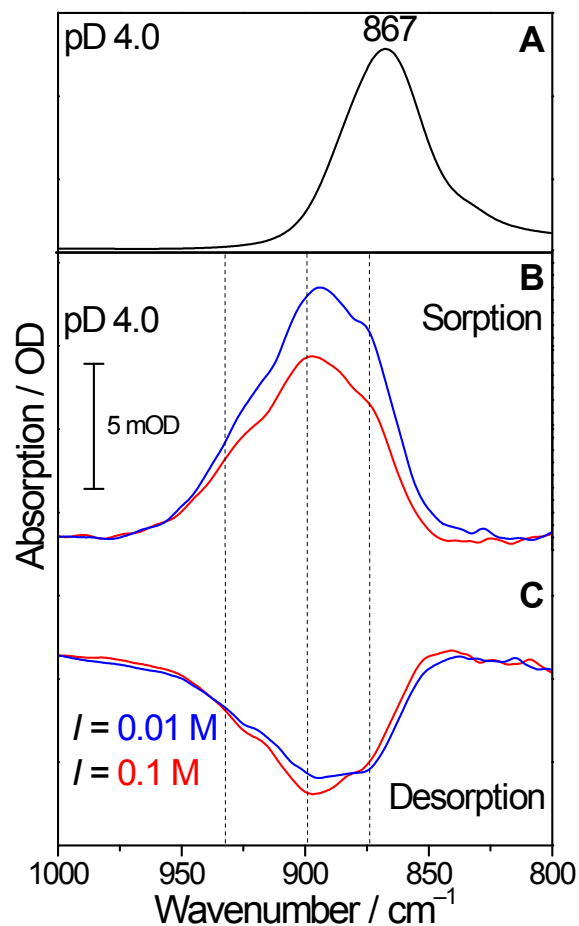


Figure S7. (a) IR spectrum of 0.1 mol·L⁻¹ selenium(VI) in aqueous solution at 0.1 mol·L⁻¹ NaCl in D₂O. (b) *In situ* IR spectra taken during selenium(VI) adsorption onto transition alumina ([Se(VI)]_{initial} = 5 × 10⁻⁴ mol·L⁻¹, D₂O, pD 4.0, 20 min of sorption, N₂) recorded at different ionic strength. (c) *In situ* IR spectrum of release of selenium(VI) (D₂O, pD 4.0, 20 min of desorption, N₂) recorded at different ionic strength after starting to flush the transition alumina phase with blank solution.

Surface complexation modeling

Site density of transition alumina

Proton active surface density is systematically underestimated by continuous titration and depends on the nature and concentration of the background electrolyte. Thus, it is more reasonable to consider site density values based on crystallographic structural information. Since Al ions are present in both hexagonal and tetrahedral coordination on the surface, the situation is rather complex for γ -Al₂O₃. The surface properties of γ -Al₂O₃ were described by Hiemstra et al.¹ considering one $\equiv\text{SO}^{-0.5}$ site (representing the acidic groups $\text{Al}^{\text{IV}}\text{OH}^{-0.25}$, $\text{Al}^{\text{IV}}\text{Al}^{\text{VI}}\text{O}^{-0.75}$ and $\text{Al}^{\text{VI}}_3\text{O}^{-0.5}$), as well as one $\equiv\text{AlOH}^{-0.5}$ with singly coordinated hydroxyl group. 25% of both types of sites were assumed to be located in the subsurface. A total site density of 6.6 sites nm⁻² (2.5 for each normal site and 0.8 for each subsurface site) was used by Hiemstra et al. A surface site density of 7 sites nm⁻², close to the total surface site density used by Hiemstra et al., was chosen in this study (as well as in the work of Mayordomo et al.²), considering only singly coordinated hydroxyl group. This approach worked quite well and it was therefore justified to avoid excessive complexity of the model. One additional initial consideration was to provide a sufficient excess in the concentration of sites compared to the maximum Se(VI) adsorption measured.

Goodness of fit

A well-known metric for the goodness of fit in FITEQL (this used to be the standard fitting software) is the so-called WSOS/DF (weighted sum of squares/ degrees of freedom) parameter. Values between 0.1 and 20 refer to a reasonably good fit, while values close to 1 relate to excellent fits, in relation to the chosen error estimates. This parameter can be strongly impacted by the assignment of the uncertainties of the experimental points as well as their weights (this is typically an issue when data from different sources are used). A similar problem exists when UCODE is coupled to FITEQL. In our case FITEQL is used as a simulation tool. The fitting software UCODE also provides a code inherent goodness of fit parameter, which can be manipulated in various ways. There is consensus that the goodness of fit is best verified in graphical illustrations. But even in such cases one may choose among solute concentrations, fractional adsorption or K_d values and obtain different results.

Here, we opted for a different approach to decide how well the model fits the data. Simulation results (% Se sorbed or zeta potential) were plotted vs. the experimental data (% Se sorbed or zeta potential with their uncertainties). A perfect fit would lead to a correlation coefficient R^2 of 1. The R^2 values are exemplarily shown in Figure S8 related to the fit of the batch sorption and zeta potential data for the TPM option.

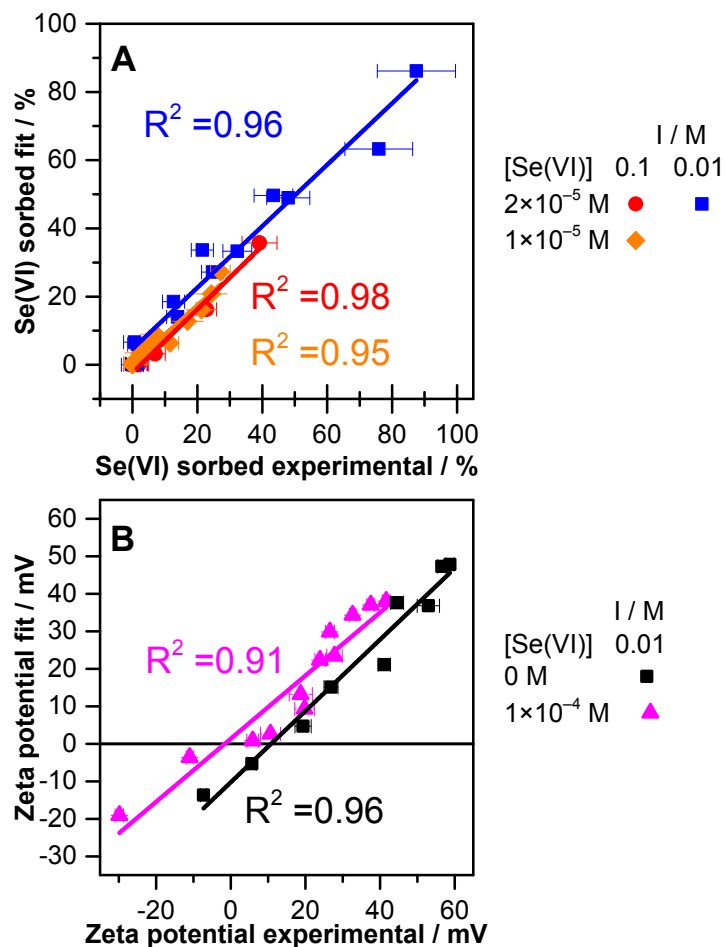


Figure S8. R^2 correlation coefficients from fitted parameters vs. experimental parameters plots for the TPM model. (A) Se(VI) sorption envelopes onto transition alumina ($[\text{Se}^{\text{VI}}]_{\text{initial}} = 1 \times 10^{-5} \text{ mol}\cdot\text{L}^{-1}$, $m/v = 0.5 \text{ g}\cdot\text{L}^{-1}$, $I = 0.1 \text{ mol}\cdot\text{L}^{-1}$ NaCl (◆)) and $[\text{Se}^{\text{VI}}]_{\text{initial}} = 2 \times 10^{-5} \text{ mol}\cdot\text{L}^{-1}$, $m/v = 1 \text{ g}\cdot\text{L}^{-1}$, $I = 0.1 \text{ mol}\cdot\text{L}^{-1}$ NaCl (●) and $I = 0.01 \text{ mol}\cdot\text{L}^{-1}$ NaCl (■). (B) Zeta potential of the surface of transition alumina ($[\text{Se}^{\text{VI}}]_{\text{initial}} = 0 \text{ mol}\cdot\text{L}^{-1}$ (■) and $1 \times 10^{-4} \text{ mol}\cdot\text{L}^{-1}$ (▲), $m/v = 0.25 \text{ g}\cdot\text{L}^{-1}$, $0.01 \text{ mol}\cdot\text{L}^{-1}$ NaCl).

As can be seen in Figure S8, all regression coefficients were higher than 0.90, meaning that the quality of the fit is very good.

Blind prediction of the literature data

A literature survey was performed and batch data related to the Se(VI)/ γ -Al₂O₃ binary system were digitized³⁻⁶. Table S1 summarizes the experimental conditions and some properties of the minerals involved in the respective investigations.

Table S1. Experimental conditions and mineral properties of the digitized batch sorption data from literature for the Se(VI)/ γ -Al₂O₃ binary system

Literature	Ionic strength (mol·L ⁻¹)	m/v (g·L ⁻¹)	Specific surface area (m ² ·g ⁻¹)	pH _{PZC} /pH _{IEP}	[Se(VI)] _{initial} (mol·L ⁻¹)
Ghosh et al. ⁵	0.1 NaCl	1	250	pH _{PZC} = 8.1	1.42 × 10 ⁻⁴
Elzinga et al. ⁴	0.01 and 0.15 NaCl	10	100	pH _{IEP} = 9.2	1 × 10 ⁻³
Boyle-Wight et al. ³	0.1 NaNO ₃	5	80	n.m.*	6 × 10 ⁻⁴
Wu et al. ⁶	0.1 NaNO ₃	30	100	pH _{PZC} = 8.3	5 × 10 ⁻³

*n.m.: not mentioned

The final model proposed in this study was used to predict the data from the literature and the outcome is shown in Figures S9 and S10.

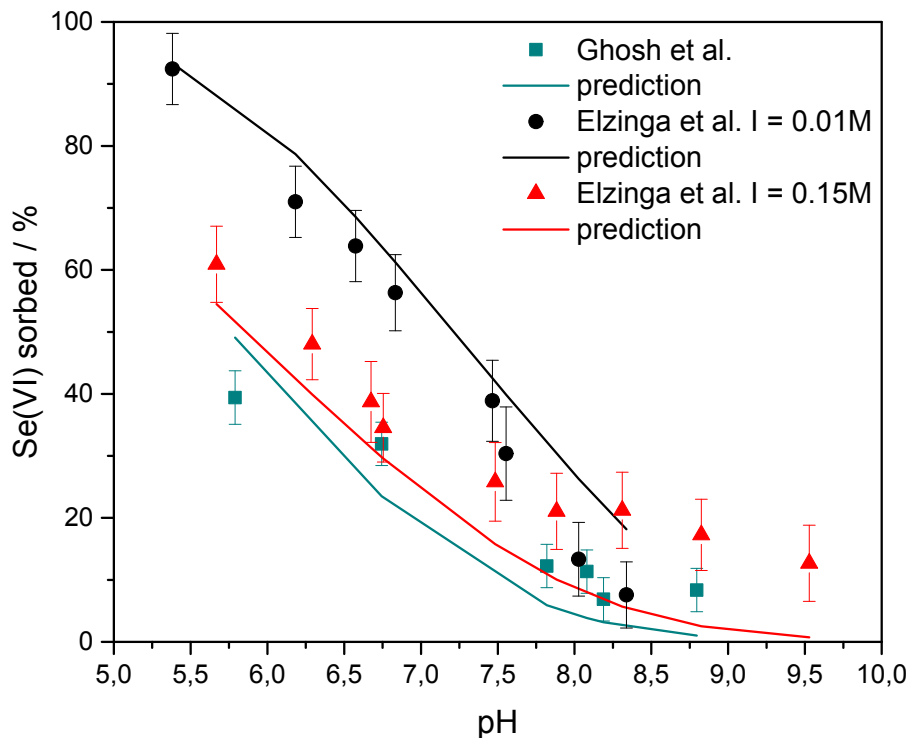


Figure S9. Predictions of the model proposed in this study for batch sorption data performed in NaCl. (■) Ghosh et al. ($[\text{Se}^{\text{VI}}]_{\text{initial}} = 1.42 \times 10^{-4} \text{ mol}\cdot\text{L}^{-1}$, $m/v = 1 \text{ g}\cdot\text{L}^{-1}$, $I = 0.1 \text{ mol}\cdot\text{L}^{-1}$), (●) Elzinga et al. ($[\text{Se}^{\text{VI}}]_{\text{initial}} = 1 \times 10^{-3} \text{ mol}\cdot\text{L}^{-1}$, $m/v = 10 \text{ g}\cdot\text{L}^{-1}$, $I = 0.01 \text{ mol}\cdot\text{L}^{-1}$), (▲) Elzinga et al. ($[\text{Se}^{\text{VI}}]_{\text{initial}} = 1 \times 10^{-3} \text{ mol}\cdot\text{L}^{-1}$, $m/v = 10 \text{ g}\cdot\text{L}^{-1}$, $I = 0.15 \text{ mol}\cdot\text{L}^{-1}$).

For the batch data obtained in NaCl, the model predicts quite well the independent results from the literature. Note that the data of Elzinga et al.⁴ at $I = 0.15 \text{ mol}\cdot\text{L}^{-1}$ show an unexpected behavior since they are higher than the data at $I = 0.01 \text{ mol}\cdot\text{L}^{-1}$ at $\text{pH} > 7.5$. Our model is calibrated on data that do not show such behavior and consequently the model is unable to produce such results. Although the pH_{PZC} (8.1) of the mineral used by Ghosh et al.⁵ is one pH unit lower than the one of the nano-transition alumina used in our study, our model works

reasonably well. Overall, our model is quite capable of predicting literature data collected in NaCl background electrolytes.

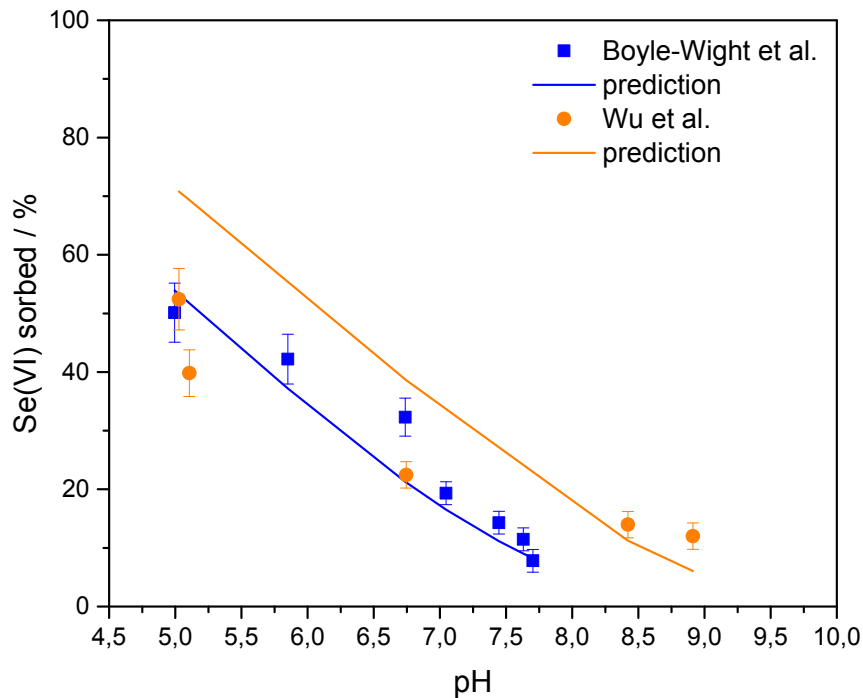


Figure S10. Predictions of the model proposed in this study for batch sorption data performed in NaNO₃. (■) Boyle-Wight et al. ($[\text{Se}^{\text{VI}}]_{\text{initial}} = 6 \times 10^{-4} \text{ mol}\cdot\text{L}^{-1}$, $m/v = 5 \text{ g}\cdot\text{L}^{-1}$, $I = 0.1 \text{ mol}\cdot\text{L}^{-1}$), (●) Wu et al. ($[\text{Se}^{\text{VI}}]_{\text{initial}} = 5 \times 10^{-3} \text{ mol}\cdot\text{L}^{-1}$, $m/v = 30 \text{ g}\cdot\text{L}^{-1}$, $I = 0.1 \text{ mol}\cdot\text{L}^{-1}$).

For batch data measured in NaNO₃, the model reasonably well predicts the results of Boyle-Wight et al.³, while the prediction of the data of Wu et al.⁶ is not good at low pH.

The $\text{pH}_{\text{PZC}}/\text{pH}_{\text{IEP}}$ of the mineral used by Boyle-Wight et al. was not mentioned, while the pH_{PZC} of the mineral used by Wu et al. is one pH unit lower than the nano-transition alumina used in our study. The exact reasons why our model does not perform so well for data acquired in NaNO₃ are

not clear at this stage. One reason might be the difference in the complexation constant of the NO_3^- and Cl^- ions, i.e. 1.4 according to Wu et al. and -0.2 in our study, respectively.

References

1. T. Hiemstra, H. Yong and W. H. Van Riemsdijk, Interfacial charging phenomena of aluminum (hydr)oxides, *Langmuir*, 1999, **15**, 5942-5955.
2. N. Mayordomo, H. Foerstendorf, J. Lützenkirchen, K. Heim, S. Weiss, U. Alonso, T. Missana, K. Schmeide and N. Jordan, Selenium(IV) Sorption Onto gamma-Al₂O₃: A Consistent Description of the Surface Speciation by Spectroscopy and Thermodynamic Modeling, *Environmental Science & Technology*, 2018, **52**, 581-588.
3. E. J. Boyle-Wight, L. E. Katz and K. F. Hayes, Macroscopic studies of the effects of selenate and selenite on cobalt sorption to γ -Al₂O₃, *Environmental Science & Technology*, 2002, **36**, 1212-1218.
4. E. J. Elzinga, Y. Z. Tang, J. McDonald, S. DeSisto and R. J. Reeder, Macroscopic and spectroscopic characterization of selenate, selenite, and chromate adsorption at the solid-water interface of γ -Al₂O₃, *J. Colloid Interface Sci.*, 2009, **340**, 153-159.
5. M. M. Ghosh, C. D. Cox and J. R. Yuanpan, Adsorption of Selenium on Hydrous Alumina, *Environmental Progress*, 1994, **13**, 79-88.
6. C. H. Wu, S. L. Lo and C. F. Lin, Competitive adsorption of molybdate, chromate, sulfate, selenate, and selenite on γ -Al₂O₃, *Colloids and Surfaces a-Physicochemical and Engineering Aspects*, 2000, **166**, 251-259.